Journal of Photonics for Energy

PhotonicsforEnergy.SPIEDigitalLibrary.org

Deconvoluting contributions of photoexcited species in polymer-quantum dot hybrid photovoltaic materials

Elsa Couderc
Matthew J. Greaney
William Thornbury
Richard L. Brutchey
Stephen E. Bradforth

SPIE.

Deconvoluting contributions of photoexcited species in polymer-quantum dot hybrid photovoltaic materials

Elsa Couderc, Matthew J. Greaney, William Thornbury, Richard L. Brutchey,* and Stephen E. Bradforth*
University of Southern California, Department of Chemistry, Los Angeles, California 90089-0482, United States

Abstract. Ultrafast transient absorption spectroscopy is used in conjunction with spectroelectrochemistry and chemical doping experiments to study the photogeneration of charges in hybrid bulk heterojunction (BHJ) thin films composed of poly[2,6-(4,4-bis(2-ethylhexyl)-4*H*-cyclopenta[2,1-*b*:3,4-*b'*]-dithiophene)-alt-4,7-(2,1,3-benzothiadiazole)] (PCPDTBT) and CdSe nanocrystals. Chemical doping experiments on hybrid and neat PCPDTBT:CdSe thin films are used to deconvolute the spectral signatures of the transient states in the near infrared. We confirm the formation and assignment of oxidized species in chemical doping experiments by comparing the spectral data to that from spectroelectrochemical measurements on hybrid and neat PCPDTBT:CdSe BHJ thin films. The deconvolution procedure allows extraction of the polaron populations in the neat polymer and hybrid thin films. © *2015 Society of Photo-Optical Instrumentation Engineers (SPIE)* [DOI: 10.1117/1.JPE.5.057404]

Keywords: bulk heterojunction; hybrid solar cell; charge transfer; ultrafast spectroscopy; chemical doping.

Paper 14077SSP received Oct. 7, 2014; accepted for publication Nov. 19, 2014; published online Jan. 2, 2015.

1 Introduction

The development of low cost, high throughput methods for processing solar cells is important for realizing the widespread deployment of photovoltaic technologies. Bulk heterojunction (BHJ) solar cells have been exploited for this purpose, with champion power conversion efficiencies (PCEs) now regularly reaching the 6% to 8% range based upon semiconducting polymers and fullerenes.[1,2] Such conjugated polymers are attractive due to their high absorption coefficients and excellent film forming properties. They are often used as the donor component in BHJs and are paired with different acceptors, such as fullerenes or semiconductor nanocrystals. The latter can offer benefits that are less easily exploited in fullerene-based acceptors such as spectral tunability through size and shape modifications, as well as high dielectric constants and high intrinsic charge carrier mobilities.[3,4] Solar cells based upon semiconducting polymers and inorganic nanocrystals form the basis for the field of hybrid photovoltaics, which has seen steady progress over the past decade and a revived interest over the past few years.[5–7]

Champion hybrid BHJ solar cells composed of conjugated polymers and lead chalcogenide nanocrystals currently reach 5.5% PCE,[8] with further understanding of the fundamental photophysical properties of these systems required to bridge the PCE gap between the all-organic photovoltaic systems and these hybrids. The external quantum efficiency of these BHJ thin films is the product of the efficiency of several individual processes; that is, light absorption, exciton dissociation, charge separation, charge transport, and charge extraction. These processes occur on several time scales ranging from as small as femtoseconds (for exciton dissociation events) up to milliseconds for complete device operation. In disordered materials like the ones typically used in BHJs, the actual times required for each photovoltaic process may depend heavily on the chemical and physical properties of the specific electron donating (e.g., polymer)

*Address all correspondence to: Richard L. Brutchey, E-mail: brutchey@usc.edu; Stephen E. Bradforth, stephen.bradforth@usc.edu

and accepting (e.g., fullerene or nanocrystal) materials.[9–15] As such, it is of interest to gain a more complete understanding about how to control and rationally tailor the chemical properties that control the photovoltaic processes in BHJ solar cells.

The photogeneration of charge carriers occurs through the dissociation of strongly bound excitons via charge transfer at the donor–acceptor interface.[16] Here, we aim to understand the charge photogeneration process and the material parameters influencing it using the hybrid polymer:nanocrystal system based on the low band gap polymer poly[2,6-(4,4-bis(2-ethylhexyl)-4*H*-cyclopenta[2,1-*b*:3,4-*b'*]-dithiophene)-alt-4,7-(2,1,3-benzothiadiazole)] (PCPDTBT, $E_{opt} \approx 1.5$ eV) in combination with CdSe nanocrystals capped with *tert*-butylthiol (tBT) surface ligands.[17,18] We have selected this specific system for two primary reasons: (i) this hybrid BHJ offers the possibility of selectively exciting one component of the junction (the donor polymer) and thus enabling specific probing of the electron transfer at the polymer:nanocrystal interface and (ii) our previous work with this system suggested the existence of ultrafast electron transfer leading to practical PCEs between 3% and 4%.[18–20]

To study the dynamics of the polymer exciton and the subsequent charge photogeneration, we use spectrally resolved ultrafast transient absorption (TA) spectroscopy.[19,21] Such an experiment consists of comparing the absorption spectrum of a material in its excited state to the absorption spectrum of this material in the ground state. The evolution of the transient states is obtained by measuring the excited state spectra at different times after the excitation pulse. The spectral and time resolutions of this type of setup can elucidate details about critical processes occurring on femtosecond time scales, making the technique invaluable for gaining a fundamental understanding about the basic photophysics in such systems. Nevertheless, in most materials, spectral bands from different transient species overlap and it can be difficult to obtain quantitative and conclusive information about specific transient species.

In an attempt to overcome the spectral congestion, we use complementary techniques to determine the spectral shapes of the different transient species. First, we use ultrafast TA of the neat PCPDTBT solution to determine the exciton absorption spectrum. Then we perform chemical doping experiments and spectroelectrochemistry to determine the absorption spectrum of the oxidized polymer. These absorption spectra constitute a basis set to deconvolute the TA spectra of the hybrid films as well as the information required to extract the polaron density.

2 Absorption Spectra of PCPDTBT Transient Species

This section presents the different techniques employed to obtain the basis set of spectra used to deconvolute the hybrid film TA spectra.

2.1 *Absorption Spectrum of PCPDTBT Excitons*

Excitons on conjugated polymers are highly bound electron–hole pairs. They have rather short lifetimes, typically on the order of tens of picoseconds for PCPDTBT films (i.e., a biexponential decay of 20 and 120 ps, as reported by Hwang et al.[22]). The short lifetimes of such excited species are quite amenable to study using ultrafast TA spectroscopy, which enables access to spectral information on these timescales.

In a typical TA experiment, the PCPDTBT polymer was selectively excited with an 800 nm pulse, pumping in the low energy tail of its $S_1 \leftarrow S_0$ transition (see Fig. 1).[23] The absorption spectrum of the sample is then measured by a broadband pulse in the near infrared (NIR, e.g., 1000 to 1400 nm) at a delay (Δt) after the pump pulse. Spectra presented here are the difference of the excited state absorption spectrum (pump on) and the ground state absorption spectrum (pump off). Due to the depletion of the ground state population, the ground state-based transitions appear negative and are designated "ground state bleach," whereas the absorption bands of the excited state appear positive and are called "photoinduced absorption (PIA) bands."

In an effort to limit the formation of interchain charge transfer states (i.e., the electron on one polymer chain and the hole on another), as is observed in neat polymer films,[19,21,22] we performed the TA measurements in solution using 1,2-dichlorobenzene (DCB). In the NIR region, the PCPDTBT solution presents a broad positive feature centered around 1400 nm (see Fig. 2).

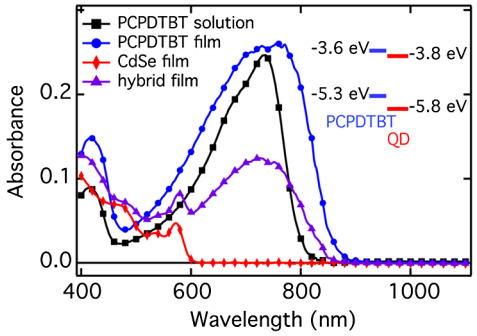

Fig. 1 Representative steady-state absorption spectra of the donor and acceptor components of the BHJs studied: PCPDTBT solution (square), PCPDTBT film (circles), CdSe nanocrystal film (diamonds), and hybrid BHJ film composed of PCPDTBT:CdSe nanocrystals (triangles). The inset shows the frontier energy levels of the PCPDTBT polymer and of the CdSe nanocrystals, which were determined by electrochemistry for each individual component.[19]

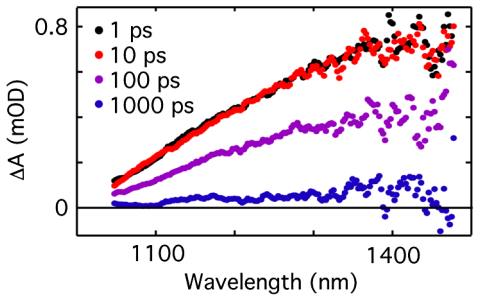

Fig. 2 Transient absorption (TA) spectra of a PCPDTBT solution for various delays between the pump and the probe pulses. $\lambda_{exc} = 800$ nm, pump fluence $= 200\ \mu J\,cm^{-2}$.

The spectral shape does not evolve in time and it decays with a 160 ps time constant. This wide band is used as the spectral signature of excitons in the following analyses.

2.2 *Absorption Spectra of Oxidized PCPDTBT*

In the hybrid BHJ studied here, the PCPDTBT acts as the electron donor. Therefore, after selective excitation of the polymer at 800 nm, exciton dissociation occurs after migration to the interface with the CdSe nanocrystals followed by electron transfer. This process leaves the polymer positively charged with spectral features indicative of polaron formation. In order to investigate the spectral signatures of the positively charged polymer, we followed previous literature examples for generating the oxidized form of PCPDTBT using $SbCl_5$ as a chemical oxidative dopant.[24] Furthermore, we compare our spectral results from chemical doping to those obtained from oxidative spectroelectrochemistry and find good agreement between the spectral features of the oxidized PCPDTBT species.

2.2.1 *Neat polymer solution*

The positive species of PCPDTBT in solution are studied by adding low weight concentrations of $SbCl_5$ to a dilute solution of polymer.[21,24] Figure 3(a) shows the steady-state absorption spectra of a series of solutions with increasing $SbCl_5$ content (from 0.1 to 1 wt% of $SbCl_5$ relative to the polymer). The intensities of the undoped state absorption bands at 400 and 720 nm are reduced in the doped form and are accompanied by the loss of some vibronic structure. Furthermore, doping leads to two additional features, i.e., (i) a shoulder at ~820 nm and (ii) a wide absorption band peaking at ~1280 nm.

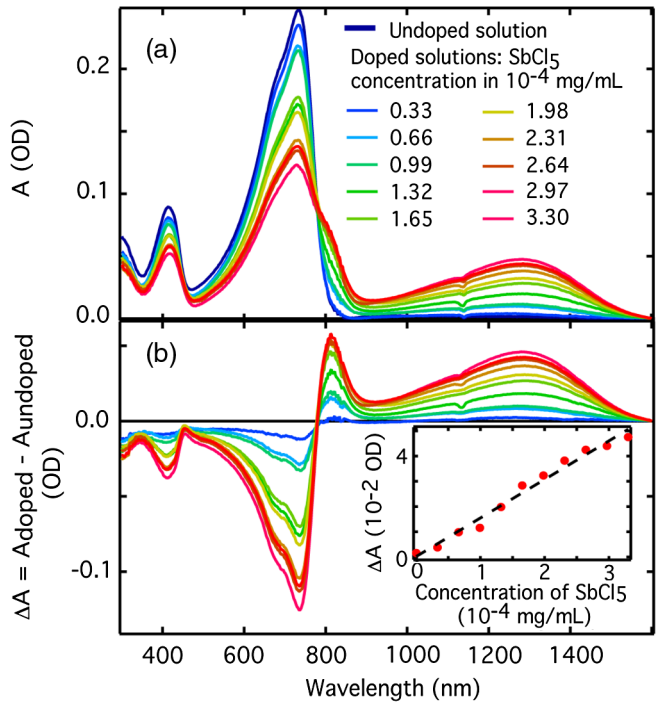

Fig. 3 (a) PCPDTBT solution steady-state absorption spectra for different $SbCl_5$ dopant concentrations using a fixed polymer concentration of 33 $\mu g\,mL^{-1}$ in DCB. (b) Difference spectra for the raw absorbance data shown in (a). The inset of (b) details the determination of the polaron absorption coefficient at 1284 nm. Measurements were taken in an integrating sphere and therefore account for scattering and reflections.

Figure 3(b) shows the difference between the undoped and doped spectra. The inset of Fig. 3(b) gives the peak absorbance ΔA (1284 nm) of the oxidized PCPDTBT polymer absorbance relative to that of the undoped polymer at 1284 nm, as a function of $SbCl_5$ ($mg\,mL^{-1}$). A linear fit was used to obtain the polaron cross-section. Assuming that each $SbCl_5$ molecule generates a polymer polaron, and with the molar mass of $SbCl_5$ ($M_{SbCl5} = 299.02\ g\,mol^{-1}$), the cross section σ is estimated as

$$\sigma = \ln(10)\frac{A_{1284\ nm}\times M_{SbCl_5}}{l\times c_m \times N_A} = 1.75\times 10^{-15}\,cm^2/\text{polaron},$$

where $l = 1$ mm (the cuvette path length) and N_A is Avogadro's number.

2.2.2 *Neat polymer film*

PCPDTBT films were doped by dipping them in a 20 ppm solution of $SbCl_5$ in acetonitrile.[21,25] The absorption spectra of thin films spin coated on quartz slides before and after doping are shown in Fig. 4(a). The steady-state absorption bands at 400 and 780 nm are reduced in intensity and lose their vibronic structure, similarly to the solution doping. A broad band also appears in the doped state, peaking around 1240 nm (i.e., a 40-nm blue shift relative to the doped polymer in solution). Here, the 820 nm shoulder does not appear explicitly. Two factors explain this difference: (i) the whole ground state absorption is already red shifted in the undoped films relative to the undoped solution and (ii) the NIR polaron band is broader than in solution.

2.2.3 *Hybrid film*

To assess the spectral shape of the oxidized polymer within the PCPDTBT:CdSe BHJ, we also doped hybrid thin films by dipping them using an analogous procedure. Here, the polymer and

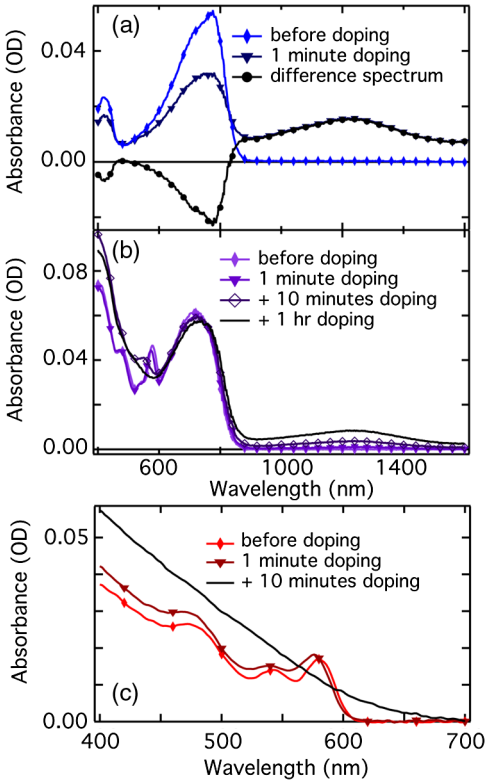

Fig. 4 (a) Absorption spectra of the PCPDTBT thin film before doping (diamond), after a 1 min dip in a 20 ppm solution of $SbCl_5$ in acetonitrile (triangles), shown together with the difference spectrum. (b) Absorption spectra of the PCPDTBT:CdSe hybrid BHJ thin film before doping (diamond), after a 1 min dip in a 20 ppm solution of $SbCl_5$ in acetonitrile (triangles); after an additional 10 min dip in the dopant solution (hollow diamonds) and finally after an additional 1 h dip in the dopant solution (line). (c) Control experiment with a neat CdSe nanocrystal film: absorption spectra of the nanocrystal thin film before doping (diamond), after a 1 min dip in a 20 ppm solution of $SbCl_5$ in acetonitrile (triangles); after an additional 10 min dip in the dopant solution (line). Measurements were taken in an integrating sphere and therefore account for scattering and reflections.

the nanocrystals are simultaneously oxidized and the large volume fraction of CdSe nanocrystals limits the dopant diffusion into the films, which results in the necessity of longer dipping times, as shown in Fig. 4(b). (For the mass fraction used here of $m_{QD}/m_{polymer} = 8$, and the CdSe and polymer volumic densities of $\rho_{CdSe} = 5.8$ g/cm^3 and $\rho_{polymer} = 1$ g/cm^3, the volume fraction occupied by QDs is around 60%.) In the hybrid BHJ film, the bleach of the polymer ground state absorption bands is less pronounced than in the neat polymer film. The shape of the NIR polaron band is similar to that observed in the neat polymer film and peaks at ~1240 nm. Interestingly, the CdSe nanocrystal excitonic transition bands observed at 475, 535, and 580 nm before doping are blue shifted before disappearing entirely upon doping. Finally, the absorbance at lower wavelengths actually increases upon doping.

In order to verify the origin of these last effects, we doped neat CdSe nanocrystal films. Figure 4(c) shows that the CdSe nanocrystal film spectra also exhibit a blue shift of the excitonic transitions upon doping, followed by a complete disappearance of the excitonic structure for prolonged doping. The loss of excitonic features is attributed to the loss of quantum confinement of the exciton and to increased disorder throughout the nanocrystal assembly due to oxidation. Here, the neat CdSe nanocrystal results indicate that the additional effects observed in the hybrid film compared to the neat polymer film are related to the nanocrystals and not to differences of the polymer oxidation itself.

To confirm our interpretation of spectra for the chemically oxidized thin films, we performed spectroelectrochemical measurements on neat PCPDTBT and hybrid PCPDTBT:CdSe BHJ films. The difference spectra for these two samples are presented in Fig. 5. The neat polymer film exhibits a bleaching of the high-energy absorption bands at ~400 and 760 nm. A positive,

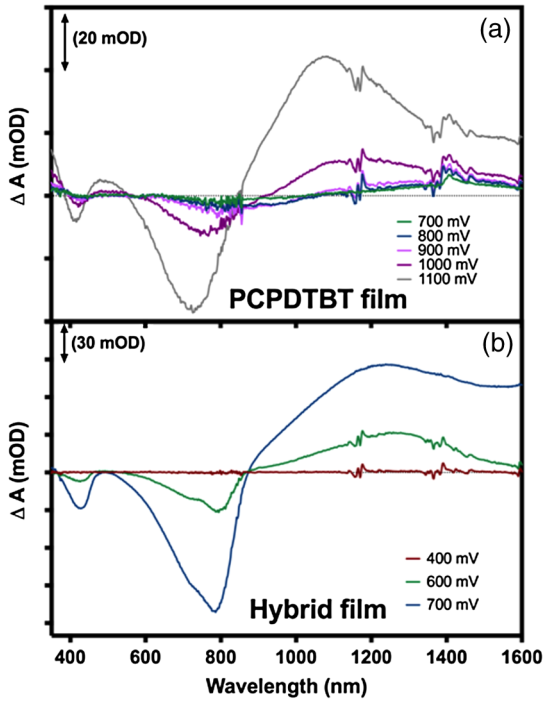

Fig. 5 Difference steady state absorption spectra obtained from spectroelectrochemical measurements on (a) neat PCPDTBT films and (b) hybrid PCPDTBT:CdSe BHJ films. The films were spun-cast onto ITO substrates, which acted as the working electrode. A Pt-wire counter electrode and Ag-wire pseudoreference electrode were used to complete the three-electrode setup. Measurements were performed in an acetonitrile solution of 0.1 M tetrabutylammonium hexafluorphosphate.

lower energy polaron feature at ~1180 nm occurs in coincidence with the high-energy bleaches. Interestingly, the polaron signal appears to blue-shift as the applied potential becomes more oxidative as evidenced by the maxima shift from ~1180 to 1110 nm upon switching from 1000 mV applied bias to 1100 mV.

The hybrid PCPDTBT:CdSe films behave similarly to the neat PCPDTBT film, with strong bleaches observed around 780 and 410 nm. These are again accompanied by a broad polaron feature in the NIR with a peak maximum of ~1200 nm. It is worth highlighting the fact that the nanocrystal bleach is not apparent in the difference spectra for the hybrid films. This is not surprising considering that PCPDTBT has a thermodynamically higher energy HOMO level than the nanocrystals and should bleach at much lower potentials than the nanocrystals.

3 Deconvolution of TA Spectra of Hybrid BHJ in the NIR

The TA spectra exhibit an overlap between the polaron and the exciton signals in the NIR range. In Fig. 6, the TA spectra of (a) a neat PCPDTBT film and (b) a PCPDTBT:CdSe BHJ film are shown for a pump–probe delay of 180 fs. The polaron contribution is visible as a shoulder around 1200 nm, where the contribution from the exciton is still very strong, illustrating the need for a deconvolution process. At this time delay, the spectra from the neat polymer and from the hybrid are very similar. Here, we compare the relative amplitudes of their exciton and polaron components. At longer time delays (c and d are for 1 ps delay; e and f are for 10 ps delay), the polaron band becomes more pronounced as the exciton band loses intensity.

We use a linear combination of the exciton spectrum determined in neat PCPDTBT solution (cyan in Fig. 6, measured in Sec. 2.1) and the polaron spectrum determined by film doping experiments (dark blue in Fig. 6, measured in Sec. 2.2.2) to deconvolute the TA signals of the neat PCPDTBT film and of a PCPDTBT:CdSe BHJ (purple). More precisely, we used a Metropolis–Hastings algorithm (Matlab Statistical Toolbox) to compare the observation d_{obs} (the TA spectrum) to the prediction from the linear combination model $d_{\text{pred}} = a\times$

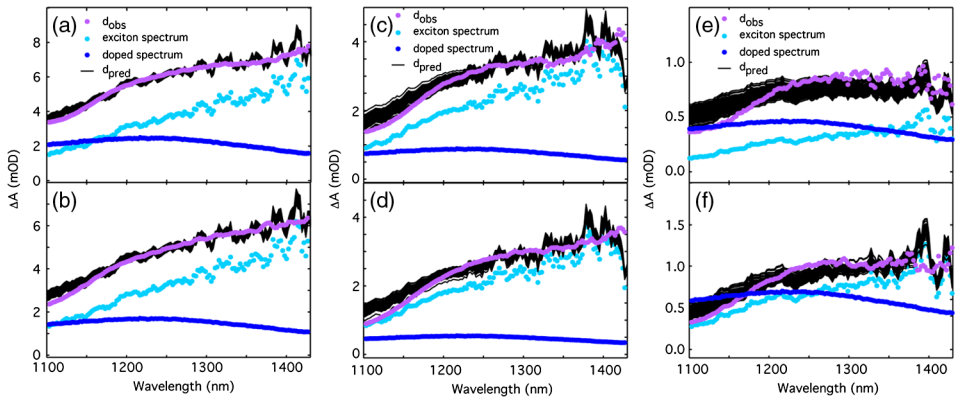

Fig. 6 Deconvolution of the TA spectra of a neat PCPDTBT film in (a, c, e) and of a PCPDTBT:CdSe BHJ film in (b, d, f). Three time delays between the pump and probe are shown: 180 fs for (a, b), 1 ps for (c, d) and finally 10 ps for (e, f). The TA spectra (d_{obs}) are shown in purple; these spectra were measured using $\lambda_{exc} = 800$ nm and a pump fluence of 25 μJ cm^{-2} and 85 μJ cm^{-2} for the polymer and the hybrid film, respectively. The fraction of 800-nm photons absorbed by the films was 14% for the polymer and 9% for the hybrid. A few examples of suitable $d_{pred} = a \times$ exciton spectrum $+ b \times$ polaron spectrum (see the text) are shown in black. In blue, the components of the most likely d_{pred} are given – in cyan the exciton spectrum $a_{mean} \times$ exciton spectrum, and in dark blue, the polaron spectrum $b_{mean} \times$ polaron spectrum.

exciton spectrum $+ b \times$ polaron spectrum, as detailed by our previously published work.[19,21] The comparison is made for a large set of (a, b) couples and the most likely parameters (a_{mean}, b_{mean}) are extracted using Bayes theorem. This method furthermore gives access to statistically meaningful error bars, taken as the width σ of the parameter distributions.

Figure 6 shows several d_{pred} values obtained with (a, b) couples chosen within the parameter distribution (black). Since d_{pred} is the sum of two experimental signals, it shows some oscillations from the experimental noise. Assuming that the polaron cross-section is identical to that extracted from solution doping experiments in Sec. 2.2.1, we can extract from parameter b the number of polarons present in the probed volume at 180 fs. In the neat PCPDTBT film, this reaches between 9×10^8 and 1.1×10^9 polarons (estimated from the width σ of the Gaussian distribution of parameter b) for 5×10^9 absorbed photons. This corresponds to a polaron yield of $20 \pm 2\%$ in the neat copolymer, similarly to what was measured in Ref. 24. In the hybrid film, the number of polarons in the probed volume reaches between 6×10^8 and 8×10^8 for 10^{10} absorbed photons.

These numbers suggest that the polaron yield is lower in the hybrid than in the polymer at short times. This seems surprising at first, especially considering that we previously showed that electron transfer is ultrafast in these PCPDTBT:CdSe BHJs.[19] However, we also showed that the majority of the transferred electrons form tightly bound pairs with the positive charge remaining on the polymer. These charge pairs possess a PIA band situated in a different wavelength range (900 to 1050 nm). In other words, the formation of tightly bound charge pairs does not result in the "usual" polymer polaron signal peaking around 1200 nm. Here, we selectively extract the number of polymer polarons that are not involved in tightly bound pairs.

4 Experimental Section

4.1 *Sample Preparation*

The sample preparation was detailed in Ref. 19. CdSe nanocrystal synthesis and tBT ligand exchange were performed as described by Greaney et al.[18] PCPDTBT was used as received from 1-Material, with a molecular weight and a polydispersity index of 28.5 kDa and 1.9, respectively. Solutions of 15 mg mL^{-1} PCPDTBT were prepared in DCB and were mixed with DCB-tetramethylurea (95:5 vol%) dispersions of CdSe nanocrystal to final concentrations of

22.5 mg mL^{-1} (2.5 mg mL^{-1} PCPDTBT, 20 mg mL^{-1} CdSe) and were stirred for 2 to 4 h in the dark prior to use. The solutions passed through 0.45 μm PTFE syringe filters and were spun-cast in air onto clean quartz slides and encapsulated by a second quartz side glued with epoxy in a nitrogen-filled glove bag.

4.2 *Solution Doping Measurements*

A stock solution of PCPDTBT in DCB was prepared with a 0.033 mg mL^{-1} concentration. Aliquots (8 μL) of $SbCl_5$ were added to obtain doping levels between 0.1 and 1 wt % (0.1 wt % increments for each 8 μl aliquot) relative to the polymer.[24] The absorption data were then corrected for the concentration changes due to the aliquot addition.

4.3 *Film Doping Experiments*

A 20 ppm solution of $SbCl_5$ in acetonitrile was prepared and placed in petri dishes in which to soak the thin films for the desired amount of time.[25]

4.4 *TA Experiments*

TA measurements were detailed in Ref. 19. Briefly, TA measurements were carried out using the output of a Coherent Legend Elite Ti:sapphire amplifier (1 kHz, 3.5 mJ, 35 fs). The amplifier output was used as the 800-nm pump pulse. Here, we use only the spectra measured in the NIR region: the white light supercontinuum probe pulses were polarized parallel to the pump pulse and generated using a rotating sapphire window. The probe pulse was dispersed by an Oriel MS1271 spectrograph onto a 256 pixel Hamamatsu InGaAs photodiode array. To obtain satisfactory signal-to-noise ratio on the optically thin samples and to compensate the different absorbances of the samples, transient spectra were measured for typical pump fluences of 25 to 85 μJ cm^2 for the polymer and hybrid films and 200 μJ cm^2 for the PCPDTBT solution. Samples were translated perpendicular to the path of the pump and probe to prevent photodamage.

4.5 *Spectroelectrochemistry*

Spectroelectrochemistry (SEC) experiments were performed using a BASi potentiostat and a Perkin-Elmer Lamba 950 UV-Vis-NIR spectrophotometer. Polymer and nanocrystal:polymer hybrid films for SEC measurements were prepared on ITO cuvette electrodes (Delta Technologies, Ltd., $\rho = 5$-15 Ω) by spin-coating from solution. The polymer or hybrid film on ITO was used as the working electrode in conjunction with a platinum counter electrode and a silver pseudoreference electrode. A solution of 0.1 M tetrabutylammonium hexafluorphosphate in acetonitrile was used to prevent dissolution of the film. An initial absorption spectrum was acquired before incrementally increasing the applied bias by 100 mV steps. The solution was allowed to reach electrochemical equilibrium at each applied bias for several minutes before acquiring the corresponding spectra.

5 Conclusions

TA spectroscopy of organic and hybrid materials for photovoltaics is widely used to identify photoexcited species and their population dynamics. Detailed analysis often suffers from the spectral congestion of the excited species signatures. In order to relate the spectroscopic observables to the excited state populations and hence to the operation of photovoltaic devices, it is, therefore, essential to deconvolute the spectral contributions of the different excited species. In this paper, we demonstrated the deconvolution of the spectral congestion observed in NIR TA measurements of PCPDTBT and its BHJ with CdSe nanocrystals by using complementary techniques, namely TA in solution to obtain the polymer exciton spectrum and spectroelectrochemistry supported by chemical doping to obtain the oxidized polymer spectra. This basis set of spectra is used to fit the polymer and the hybrid TA data using the Bayes theorem and a

Metropolis algorithm to extract statistically relevant error bars that take into account both the uncertainties in the data and the uncertainties of the model. Such a procedure allows extraction of polaron populations in the neat polymer film and in the hybrid films. In turn, this analysis supports the conclusion that 800-nm excitation of the hybrid results mainly in bound polarons pairs, as is consistent with our previous study.[19] This type of procedure could be applied to other types of photovoltaic materials and should help the quantitative understanding of the operation of thin film photovoltaic device operation from spectrally resolved PIA signals.

Acknowledgments

M.J.G., R.L.B., and the spectroelectrochemistry experiments were supported by the National Science Foundation under DMR-1205712. E.C., S.E.B., and the ultrafast TA measurements were supported as part of the Center for Energy Nanoscience, an Energy Frontier Research Center funded by the U.S. Department of Energy, Office of Science, Office of Basic Energy Sciences under Award Number DE-SC0001013.

References

1. Y.-W. Su, S.-C. Lan, and K.-W. Wai, "Organic photovoltaics," *Mater. Today* **15**(12), 554–562 (2012).
2. M.C. Scharber and N. S. Sariciftci, "Efficiency of bulk-heterojunction organic solar cells," *Prog. Poly. Sci.* **38**(12), 1929–1940 (2013).
3. W. U. Huynh, J. J. Dittmer, and A. P. Alivisatos, "Hybrid nanorod-polymer solar cells," *Science* **295**(5564), 2425–2427 (2003).
4. T. Xu and Q. Qiao, "Conjugated polymer-inorganic semiconductor hybrid solar cells," *Energy Environ. Sci.* **4**, 2700–2720 (2011).
5. M. J. Greaney and R. L. Brutchey, "Ligand engineering in hybrid polymer:nanocrystal solar cells," *Mater. Today* (2014).
6. M. Wright and A. Uddin, "Organic-inorganic hybrid solar cells: a comparative review," *Sol. Energ. Mater. Sol. Cells* **107**, 87–111 (2012).
7. F. Gao, S. Ren, and J. Wang, "The renaissance of hybrid solar cells: progresses, challenges, and perspectives," *Energy Environ. Sci.* **6**, 2020–2040 (2013).
8. Z. Liu et al., "High-efficiency hybrid solar cells based on polymer/ PbSxSe1-x nanocrystals benefiting from vertical phase segregation," *Adv. Mater.* **25**(40), 5772–5778 (2013).
9. Z. Li et al., "Comparison of the operation of polymer/fullerene, polymer/polymer, and polymer/nanocrystal solar cells: a transient photocurrent and photovoltage study," *Adv. Funct. Mater.* **21**(8), 1419–1431 (2011).
10. M. D. Heinemann et al., "Photo-induced charge transfer and relaxation of persistent charge carriers in polymer/nanocrystal composites for applications in hybrid solar cells," *Adv. Funct. Mater.* **19**(23), 3788–3795 (2009).
11. F. S. F. Morgenstern et al., "Ultrafast charge- and energy-transfer dynamics in conjugated polymer: cadmium selenide nanocrystal blends," *ACS Nano* **8**(2), 1647–1654 (2014).
12. H. Nagaoka et al., "Size-dependent charge transfer yields in conjugated polymer/quantum dot blends," *J. Phys. Chem. C* **118**, 5710–5715 (2014).
13. F. Gao et al., "Trap-induced losses in hybrid photovoltaics," *ACS Nano* **8**(4), 3213–3221 (2014).
14. S. Dayal et al., "The effect of nanoparticle shape on the photocarrier dynamics and photovoltaic device performance of poly(3-hexylthiophene):CdSe nanoparticle bulk heterojunction solar cells," *Adv. Funct. Mater.* **20**(16), 2629–2635 (2010).
15. U. Cappel et al., "Charge generation dynamics in CdS:P3HT blends for hybrid solar cells," *J. Phys. Chem. Lett.* **4**(24), 4253–4257 (2013).
16. A. J. Moule et al., "Hybrid solar cells: basic principles and the role of ligands," *J. Mater. Chem.* **22**, 2351–2368 (2012).
17. D. H. Webber and R. L. Brutchey, "Ligand exchange on colloidal CdSe nanocrystals using thermally labile tert-butylthiol for improved photocurrent in nanocrystal films," *J. Am. Chem. Soc.* **134**(2), 1085–1092 (2012).

18. M. J. Greaney et al., "Improving open circuit potential in hybrid P3HT:CdSe bulk heterojunction solar cells via colloidal tert-butylthiol ligand exchange," *ACS Nano*, **6**(5), 4222–4230 (2012).
19. E. Couderc et al., "Direct spectroscopic evidence of ultrafast electron transfer from a low band gap polymer to CdSe quantum dots in hybrid photovoltaic thin films," *J. Am. Chem. Soc.* **135**(49), 18418–18426 (2013).
20. M. J. Greaney et al., "Novel semi-random and alternating copolymer hybrid solar cells utilizing CdSe multipods as versatile acceptors," *Chem. Commun.* **49**(77), 8602–8604 (2013).
21. E. Couderc et al., "Ultrafast electron transfer from low band gap conjugated polymer to quantum dots in hybrid photovoltaic materials," *Proc. SPIE* **9165**, 91650P (2014).
22. I.-W. Hwang et al., "Ultrafast electron transfer and decay dynamics in a small band gap bulk heterojunction material," *Adv. Mater.* **19**(17), 2307–2312 (2007).
23. G. Grancini et al., "Hot exciton dissociation in polymer solar cells," *Nature Mater.* **12**(1), 29–33 (2013).
24. R. Tautz et al., "Structural correlations in the generation of polaron pairs in low-band gap polymers for photovoltaics," *Nature Commun.* **3**, 970 (2012).
25. D. Herrmann et al., "Role of structural order and excess energy on ultrafast free charge generation in hybrid polythiophene/Si photovoltaics probed in real time by near-infrared broadband transient absorption," *J. Am. Chem. Soc.* **133**(45), 18220–18233 (2011).

Elsa Couderc received her MS degree in condensed matter physics from the École Normale Supérieure in 2008 and her PhD in material physics from the Commisariat à l'Énergie Atomique in 2011. She then joined the University of Southern California as a postdoctoral researcher. Her main research interest lies in charge transfer and charge transport within disordered nanostructures.

Matthew J. Greaney received his BS in chemistry from the University of California, Berkeley, in 2006 working with T. Don Tilley and his MS in chemistry from the University of San Francisco in 2010 with Larry Margerum. He is currently a PhD candidate in the Brutchey group at the University of Southern California, where he studies the synthesis and surface chemistry of semiconductor nanocrystals for photovoltaic applications.

William Thornbury is an undergraduate researcher at the University of Southern California.

Richard L. Brutchey received his BS in chemistry from the University of California, Irvine, and his PhD in chemistry from the University of California, Berkeley. After a postdoctoral fellowship at the University of California, Santa Barbara, he began his independent career in 2007 at the University of Southern California, where he is currently an associate professor of chemistry. The Brutchey group focuses on the design of rational synthetic routes to colloidal inorganic nanocrystals for use in solar energy conversion and energy storage applications.

Stephen E. Bradforth is professor and chairman at the Department of Chemistry at the University of Southern California. He received his BA from Cambridge University in 1987 and his PhD from the University of California, Berkeley, in 1992, and carried out postdoctoral work at the University of Chicago. His research involves applying ultrafast spectroscopy to problems in DNA damage, aqueous phase ionization and reactivity, and characterizing light harvesting in molecular and nanoparticle based materials for solar energy.